ELSEVIER

Nuclear Instruments and Methods in Physics Research A 422 (1999) 428–432

NUCLEAR INSTRUMENTS & METHODS IN PHYSICS RESEARCH Section A

Experimental characterization of low-energy X-ray semiconductor detectors

M.C. Lépy[a,*], J.L. Campbell[b], J.M. Laborie[a], J. Plagnard[a], P. Stemmler[c], W.J. Teesdale[b]

[a] *CEA/DAMRI-BNM/Laboratoire Primaire des Rayonnements Ionisants, B.P. 52, F-91193 Gif-sur-Yvette Cedex, France*
[b] *University of Guelph, Guelph, Ontario, Canada NIG 2W1*
[c] *CEA/DAM-DRIF/DCRE/Service Diagnostics Expérimentaux, B.P. 52, F-91680 Bruyères-le-Châtel, France*

Abstract

Six semiconductor detectors (Si(Li) and HPGe) are calibrated in the 1–10 keV energy range by means of tunable monochromatized synchrotron radiation. Significant improvement in the quality of the response is observed in very recent detectors. A peak shape calibration is established using a modified Hypermet-type function to model the detector response for each energy step; a strong enhancement of the peak tail is shown above the binding energy for each detector material. Fano factors for both semiconductor materials are experimentally derived. This characterization will allow the improved processing of low-energy X-ray spectra by providing the intrinsic response of either kind of detector.

Keywords: Semiconductor detectors; Low-energy X-ray spectra

1. Introduction

Owing to their excellent energy resolution, semiconductor detectors play a major role in energy dispersive spectroscopy of photons. With its high density, germanium is traditionally used for high-energy spectrometry; its frontal absorbing dead layers has tended to reduce its use for low energies. The silicon detector is then preferably employed in the soft X-ray energy region. However, as a result of manufacturing technology improvements, dead layers of germanium detectors are becoming thinner thus allowing these devices to detect lower energies; moreover, as the Fano factor of germanium is lower than that of silicon, better resolution is expected. It is important both in automatic spectrum analysis programs and traditional spectrometry to carefully characterize the response of the detector for each specific measurement. This must include both the efficiency and the peak shape calibration as they depend on the incident energy. A number of experimental studies concerning the response of silicon detectors in the 1–10 keV energy range have been published in the last few years [1–3]. However, as they have not yet been used in this energy range no such information is available

* Corresponding author. Tel.: + 33 1 69 08 47 75; fax: + 33 1 69 08 95 29; e-mail: marie-christine.lepy@cea.fr.

0168-9002/99/$ – see front matter
PII: S0168-9002(98)01111-5

for the germanium detectors. It has been shown that tunable monochromatized synchrotron radiation is a very convenient tool for examining the response of a photon detector versus the incident energy [2]. It is thus worth using this source to compare performances of silicon and germanium detectors.

2. Experimental arrangement

2.1. Calibration setup

The experimental arrangement has been previously described [2]. It uses the beam line SB3 of the storage ring Super ACO, at the Laboratoire pour l'Utilisation du Rayonnement Electromagnétique (LURE), in Orsay, France. The calibration station is inside a vacuum chamber and includes a double crystal monochromator which selects a monoenergetic radiation in the continuous synchrotron beam. The detector to be calibrated is set at the end of the beam line, and the selected radiation impinges on the detector window connected to the vacuum of the calibration chamber. The detector can be moved in the plane orthogonal to the incident radiation: this allows checking that the beam arrives exactly at the center of the active crystal. A reference proportional counter (PC) can be interposed in the monoenergetic radiation path to measure the incident beam intensity. Two kinds of characterization can then be performed. First, the efficiency calibration is obtained by comparing, for the same monoenergetic radiation, the count rates on the detector and on the PC, whose efficiency is easily computed. This comparative method can also be used to study the discontinuities at the absorption edges of the detector materials and to determine the thickness of the absorbing layers in front of the crystal active volume. Second, the study of the spectrum shape versus energy allows characterization of the response of the detector to each monoenergetic line.This shape calibration is mainly of interest for processing complex X-ray spectra.

2.2. Detector characteristics

Six different detectors are characterized using the above setup. They use two kinds of semiconductor material: lithium-drifted silicon (Si(Li)) and high-purity germanium (HPGe). They are all equipped with an entrance window: these are traditional beryllium or special "low-energy" windows consisting of a light element polymer on a grid. These low-thickness, vacuum-tight windows are often limited to small diameter crystals. Some simple characteristics are measured using 6 keV monoenergetic radiation: they give information about the ability of the detector to separate two close lines and to detect low-intensity peaks. The resolution (FWHM) of the main peak is determined by fitting its shape by a Gaussian function. The peak-to-background ratio is the ratio of the intensity of the peak to the mean intensity measured in

Table 1
Characteristics of the studied detectors

Detector number	Si(Li) 1	Si(Li) 2	Si(Li) 3	Si(Li) 4	HPGe 5	HPGe 6
Active area	30 mm^2	30 mm^2	12 mm^2	12 mm^2	10 mm^2	20 mm^2
Thickness (mm)	5	3	3	3	2.5	5
Window material	Beryllium	Beryllium	Beryllium	Beryllium	Composite	Composite on a Si grid
Window thickness	10 μm	25μm	7.5 μm	10 μm		
Contact	Au	Not given	Au – 20 nm	Au	Not given	Not given
Assumed dead layer	No		Si – 0.2 μm	No		
FWHM at 6 keV	161 eV	138 eV	140 eV	170 eV	113 eV	147 eV
Peak-to-background (6 keV)	1870	25 800	2500	3650	15 900	8200
FWHM with ^{55}Fe	165 eV	140 eV	Not measured	171 eV	115 eV	148 eV
Peak-to-background (^{55}Fe)	680	14 080	Not measured	2970	10 800	3540
Peak-to-valley (^{55}Fe)	330	490	Not measured	280	620	390

the 900–1100 eV energy range. Both characteristics are also obtained using a traditional ^{55}Fe source. The corresponding performances are slightly different from those obtained with the monochromatic radiation, due to the complex shape of the ^{55}Fe spectrum [1]. A further characteristic is the peak-to-valley ratio: like resolution, it indicates the ability distinguish overlapping peaks, taking account of the peak tailing (s), far from the peak center. Individual characteristics are given in Table 1.

3. Spectra processing

3.1. Qualitative description

As there are different resolution and peak-to-background ratios, it is worth examining the relevant peak shapes in detail. In general, for a monoenergetic radiation, three main components are distinguished in the spectrum: the peak itself, its tailing and a low-energy background. The general peak shape is Gaussian, and its width depends on the energy. The peak tailing is highly dependent on the technology of the detector and its electrical contact. For the oldest Si(Li) detectors, there is a strong enhancement of the low-energy tail intensity above the silicon K binding energy, attributed to a "partially active dead layer": at the silicon discontinuity, the depth penetration is significantly reduced and the incoming photon interacts very close to the contact layer and part of the secondary electrons are lost [3]. For germanium detector 6, the peak shape has been recorded for energies just around K (11.10 keV) and L (1.22–1.25 and 1.41 keV) binding energies: in any case, the same change is noted as the spectrum background is enhanced. Moreover, for energies above the K binding energy, a germanium fluorescence peak appears which would indicate the presence of a true front dead layer. The background is attributed to events corresponding to escape of both photo-electrons and Auger electrons to and from the contact layer. This has been experimentally confirmed as in most recent detectors it is possible to distinguish the corresponding edges [4]. Finally, for photon energies above the binding energies, the spectrum also includes escape peak (s): the silicon K escape peak is 1.74 keV under the main peak, with an intensity of about 1% in the 1–5 keV energy range; in the same region, the germanium L escape is about 1.1 keV under the main peak with a relative intensity of about 1%, whereas for energies above 11.1 keV, the Kα and Kβ escape peaks intensity represents about 10% of that of the main peak, and rises, respectively, at energies 9.9 and 11 keV below the main peak. The shape of the silicon K escape peak is quite complex and strongly asymmetric as it contains silicon satellite lines [1]. The case of germanium L escapes is still more complicated as it includes Lα, Lβ and Lγ lines.

3.2. Mathematical fitting

To derive more information about the detector response and to establish its shape calibration, it is usual to fit a mathematical function to experimental data. This is currently done using a Hypermet-type function [5], including a main peak, tail(s) and background. In this work, the COLEGRAM software [6] fits the so-called "XLOW" function, taking account of a possible strong truncated step above the semiconductor binding energy:

$$\mathrm{XLOW}(E) = G(E) + T(E) + S(E) + \mathrm{ST}(E),$$

where $G(E)$ is the Gaussian part of the peak, T(E) an exponential tailing, $S(E)$ a continuous step and ST(E) the truncated step. This function is well adapted to the case of X-ray lines in silicon detectors with quite high low-energy tailing but is no longer optimal for the recent detectors where background is very low and reveals different continuous shapes that reflect electron transport between the detector, its contact and any dead layer [4]. However, the spectra are processed with this well-established function, the parameters relative to the peak width and to the tail intensity remaining pertinent: only the continuous part of the tail, $S(E)$ does not have exactly the right shape, nevertheless its mean amplitude gives useful information.It must be noted that the truncated step, ST(E) need not be included for germanium detectors nor for higher energies in the case of silicon detectors. Fig. 1 shows the intensity of the tail area relative to that of the total peak for two detectors, with the marked

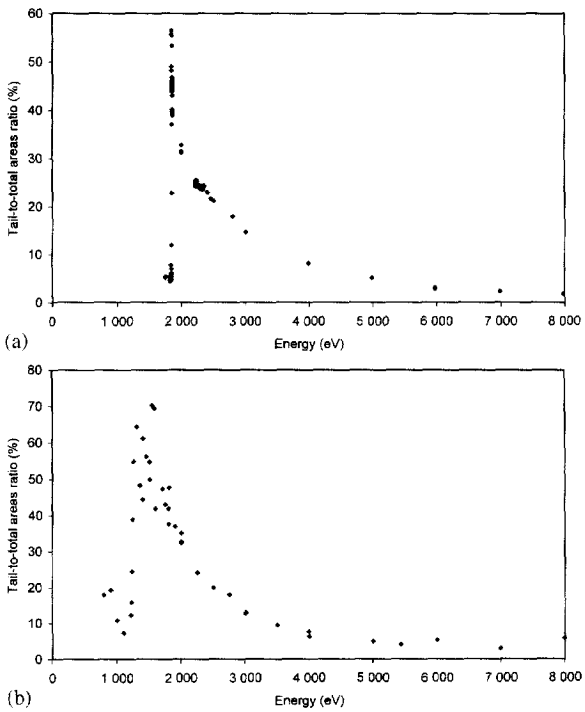

Fig. 1. Relative intensity of the tail area $(T(E) + S(E) + ST(E)$ to the total peak area (XLOW(E)) for Si(Li) detector number 3 (a) and for HPGe detector number 6 (b).

enhancement of its contribution above the semiconductor binding energy.

4. Fano factor

It is generally admitted that the peak width includes two main contributions: a constant part mainly due to electronic noise and an energy-dependent component resulting from the statistical scattering of the number of charge carriers created in the bulk of the semiconductor. The statistical variation of the number of electron–hole pairs depends on the incident energy, on the Fano factor of the semiconductor material, F, and on the mean pair creation energy w. The standard deviation of the Gaussian representing the main part of the relevant peak, can then be expressed as a function of the energy, E:

$$\sigma^2(E) = \sigma_0^2 + FwE.$$

Thus, for each studied detector, the linear fitting of σ^2 versus the energy allows deriving the value of Fw. Assuming no significant variation of Fw in the 1–10 keV energy range, Table 2 shows the values obtained using the present experimental arrangement with the combined standard uncertainties in parenthesis. Moreover, with the hypothesis of a constant pair creation energy of 3.81 eV for silicon and 2.97 eV for germanium (at the detector working temperature of 77 K), the relevant Fano factors are, respectively, between 0.106 (detector 1) and 0.120 (detector 3), and 0.099 (detector 5) and 0.108 (detector 6). Table 3 compares some recent measurements and computations of Fw for the 1–10 keV energy range. The present silicon mean value is consistent with previously published data, however, for germanium, it appears rather lower. As different kinds of detectors (CCD, Si(Li), ...) are used at different temperatures and for different incident energies, it is difficult to draw any conclusion

Table 3
Comparison of some Fw values

	Silicon	Germanium
This study (weighted mean value)	0.426 (15)	0.304 (12)
Alig [9] (Computation)	0.411	0.377
Owens [7] (170 K)	0.49	–
Croft [10] (77 K)	–	0.333
Lowe [11] (77 K)	0.4423 (4)	0.317

Table 2
Resolution compounds of the studied detectors

Detector number	Si(Li) 1	Si(Li) 2	Si(Li) 3	Si(Li) 4	HPGe 5	HPGe 6
σ_0^2	2250 (15)	911 (56)	748 (6)	2671 (10)	530 (7)	2085 (16)
Fw	0.4070	0.4240	0.4571	0.4236	0.2953	0.3208
	(48)	(108)	(52)	(25)	(16)	(23)

from the scarce published data. It would thus be of interest to perform systematic measurements to improve our knowledge of both the pair creation energy and the Fano factor for the two semiconductors.

5. Conclusions

This summary of the characteristics of some low-energy semiconductor detectors points out the wide range of response quality that can be achieved in the current experimental setups. These results have to be weighted by the detector size, as the efficiency can be a major parameter, depending on the objective of the experiment. Moreover, the technology is still evolving and the presented characteristics are expected to be improved in the near future. As stated above, the classical mathematical model appears insufficient to accurately describe spectra obtained with the most recent detectors: a more sophisticated mathematical description would require the inclusion of shapes due to weak physical effects such as escape electron humps. Monte Carlo simulations will help to accurately describe these phenomena [4], leading to the better understanding of the secondary electrons interaction in the different parts of the detectors. To our knowledge, this study is one of the first characterizations of germanium detectors in the soft X-ray range and their capability is clearly demonstrated; however, as their use in the low-energy region is new, complementary experimental studies need to be undertaken to obtain their detailed response with special attention to the vicinity of the germanium K and L binding energies. This information will be of major interest in the study of complex X-ray spectra, taking account of secondary phenomena such as radiative Auger effect and satellite lines [1]. Germanium detectors could be further used in X-ray emission analysis systems and their automated software suites, to take advantage of their superior resolution and excellent overall response.

References

[1] J.L. Campbell, J.A. Maxwell, T. Papp, G. White, X-ray Spectrom. 26 (1997) 223.
[2] M.C. Lépy, J. Plagnard, P. Stemmler, G. Ban, L. Beck, P. Dhez, X-ray Spectrom. 26 (1977) 195.
[3] F. Schloze, G. Ulm, Nucl. Instr. and Meth. A 339 (1994) 49.
[4] J.L. Campbell, G. Cauchon, M.C. Lépy, L. McDonald, J. Plagnard, P. Stemmler, W.J. Teesdale, G. White, Nucl. Instr. and Meth. submitted,.
[5] G.W. Philips, K.M. Marlow, Nucl. Instr. and Meth. 137 (1976) 525.
[6] H. Ruellan, M.C. Lépy, M. Etcheverry, J. Plagnard, J. Morel, Nucl. Instr. and Meth. A 369 (1996) 651.
[7] A. Owens, G.W. Fraser, A.F. Abbey, A. Holland, K. McCarthy, A. Keay, A. Wells, Nucl. Instr. and Meth. A 382 (1996) 503.
[8] M.C. Lépy, M.M. Bé, J. Plagnard, AIP Conf. Proc. 392 (1997) 1067.
[9] R. Casanova Alig, Phys. Rev. B 27 (2) (1983) 968.
[10] S. Croft, D.S. Bond, Appl. Radiat. Isot. 42 (311) (1991) 1009.
[11] B.G. Lowe, Nucl. Instr. and Meth. A 399 (1997) 354.